Taylor & Francis
Taylor & Francis Group

ORIGINAL ARTICLE

⚷ OPEN ACCESS

# Probabilistic treatment planning for pancreatic cancer treatment: prospective incorporation of respiratory motion shows only limited dosimetric benefit

Eelco Lens[a], Alexis N. T. J. Kotte[b], Ajay Patel[b], Hanne D. Heerkens[b], Matthieu Bal[c], Geertjan van Tienhoven[a], Arjan Bel[a], Astrid van der Horst[a] and Gert J. Meijer[b]

[a]Department of Radiation Oncology, Academic Medical Center, University of Amsterdam, Amsterdam, The Netherlands; [b]Department of Radiotherapy, University Medical Center Utrecht, Utrecht, The Netherlands; [c]Philips Healthcare, Eindhoven, The Netherlands

**ABSTRACT**

**Background:** We introduced a probabilistic treatment planning approach that prospectively incorporates respiratory-induced motion in the treatment plan optimization. The aim of this study was to determine the potential dosimetric benefit by comparing this approach to the use of an internal target volume (ITV).

**Material and method:** We retrospectively compared the probabilistic respiratory motion-incorporated (RMI) approach to the ITV approach for 18 pancreatic cancer patients, for seven simulated respiratory amplitudes from 5 to 50 mm in the superior-inferior (SI) direction. For each plan, we assessed the target coverage (required: $D_{98\%} \geq 95\%$ of 50 Gy prescribed dose). For the RMI plans, we investigated whether target coverage was robust against daily variations in respiratory amplitude. We determined the distance between the clinical target volume and the 30 Gy isodose line (i.e. dose gradient steepness) in the SI direction. To investigate the clinical benefit of the RMI approach, we created for each patient an ITV and RMI treatment plan for the three-dimensional (3D) respiratory amplitudes observed on their pretreatment 4D computed tomography (4DCT). We determined $D_{mean}$, $V_{30Gy}$, $V_{40Gy}$ and $V_{50Gy}$ for the duodenum.

**Results:** All treatment plans yielded good target coverage. The RMI plans were robust against respiratory amplitude variations up to 10 mm, as $D_{98\%}$ remained $\geq 95\%$. We observed steeper dose gradients compared to the ITV approach, with a mean decrease from 25.9 to 19.2 mm for a motion amplitude of 50 mm. For the 4DCT motion amplitudes, the RMI approach resulted in a mean decrease of 0.43 Gy, 1.1 cm³, 1.4 cm³ and 0.9 cm³ for the $D_{mean}$, $V_{30Gy}$, $V_{40Gy}$ and $V_{50Gy}$ of the duodenum, respectively.

**Conclusion:** The probabilistic treatment planning approach yielded significantly steeper dose gradients and therefore significantly lower dose to surrounding healthy tissues than the ITV approach. However, the observed dosimetric gain for clinically observed respiratory motion amplitudes for this patient group was limited.

In pancreatic cancer treatment, pretreatment multi-modality imaging enables for precise target definition and image-guided radiation therapy allows for accurate positioning of the patient. For example, by using daily cone beam computed tomography (CBCT) scans together with intratumoral fiducials, the uncertainties due to interfractional position variations of the tumor can be reduced substantially [1,2]. An important remaining uncertainty is the respiratory-induced tumor motion [3].

Using an internal target volume (ITV) based on a single four-dimensional (4D)CT measurement to account for the respiratory motion is highly conservative and could lead to unnecessary high doses to surrounding organs at risk (OARs) [4]. Alternatively, gating or real-time tracking of the tumor could be used. These procedures can yield good results, but are also technically challenging and not possible on all treatment machines [5,6].

Another approach would be to prospectively incorporate the respiratory-induced tumor motion directly into the treatment plan optimization process to achieve an optimal, patient-specific solution given the respiratory motion. This way the margins related to respiratory motion could be omitted. To apply this method, an adaptation of the treatment planning system as well as information about the expected tumor motion is needed. Several groups have proposed such adaptations to account for geometric uncertainties [7–13]. These methods mainly focused on systematic and interfractional uncertainties. In addition, all clinical data used to evaluate the methods were for prostate cancer patients and none showed the practicability for respiratory motion of abdominal tumors. Jin et al. showed that delivering an inhomogeneous dose distribution to lung tumors can result in a steeper dose gradient around the target volume in the presence of respiratory motion [14]. Inverse treatment

---

planning while prospectively incorporating the respiratory motion has been shown to be beneficial, but this has only been demonstrated in a limited number of lung cancer patients and only in a single liver cancer patient [15–17]. Therefore, clear evidence of the dosimetric benefit of using probabilistic planning for gastrointestinal tumors is still lacking. To determine the potential dosimetric benefit, probabilistic planning should be systematically compared to a margin-based approach for a larger patient cohort and a large range of respiratory motion amplitudes. Also, before probabilistic planning can be used in the clinic, its robustness against variations in the respiratory motion must be investigated.

We developed a probabilistic treatment planning approach that prospectively accounts for the respiratory-induced motion of upper abdominal tumors in the optimization process. This respiratory motion-incorporated (RMI) approach was tested and compared to the ITV approach in a group of pancreatic cancer patients using a wide range of simulated and clinically observed motion amplitudes. The goal of this study was to investigate whether the RMI approach yielded clinically acceptable plans that were robust against changes in respiratory motion amplitude. In addition, we investigated the potential dosimetric benefit of the RMI approach compared to the ITV approach.

## Material and methods

### Treatment plan optimization incorporating target motion

A plugin was developed for the Pinnacle (version 9.710) treatment planning software that incorporates respiratory-induced tumor motion directly into the optimization process of the inversely optimized treatment planning. The blurring of the dose distribution with respect to the target volume as a result of the respiratory-induced motion is taken into account when determining the optimal dose distribution. This way, a static dose distribution is calculated that when delivered to the moving target, and thus convoluted with the respiratory motion kernel, will result in that optimal dose distribution. The used technique was similar to that described in previous studies [7–13]. A detailed description of the implemented algorithm is given in the Supplementary Material.

### Patient cohort and treatment planning

To evaluate the developed RMI approach and compare it to the ITV approach, we retrospectively studied a cohort of 18 patients who were diagnosed with resectable or borderline resectable pancreatic cancer. All patients had 2–4 intratumoral gold fiducial markers, had received a pretreatment 4DCT scan and had tumor volumes ranging from 20 to 102 cm$^3$ (mean 53 cm$^3$). The tumor of patients 5, 11 and 18 was located in the pancreatic body, body/tail and tail, respectively; all other tumors were located in the pancreatic head.

All created treatment plans were inversely optimized intensity-modulated radiotherapy (IMRT) plans using 10 MV photons with beams from seven gantry angles divided evenly over a full 360° arc. For all plans, the prescription dose to

the planning target volume (PTV) was set to 50 Gy. For the RMI plans this PTV was the clinical target volume (CTV), whereby the CTV comprised the gross tumor volume plus a 5-mm margin for microscopic spread. The ITV was created by expanding the CTV anisotropically using the corresponding respiratory-induced motion amplitude [18]. In this study, both the CTV-to-PTV and the ITV-to-PTV margin were set to 0 mm because we only considered the uncertainties due to respiratory motion. As a result, we directly used the ITV and the CTV as the PTV for the ITV and RMI approach, respectively.

The following objectives were used for optimization: a $D_{max}$ of 51 Gy to the PTV [weight ($w$) = 10], $D_{min}$ of 50 Gy to the CTV ($w = 10$), and $D_{max}$ of 35 Gy to a 15-mm thick shell that was created at an isotropic distance of 6 mm around the PTV ($w = 1$).

### Simulated motion amplitudes

First, we investigated the robustness of the RMI approach against daily variations in tumor motion. Second, we systematically determined the potential dosimetric benefit of the RMI approach compared to the ITV approach. Both the robustness and dosimetric benefit were investigated using treatment plans based on seven simulated respiratory motion amplitudes up to 50 mm. The seven respiratory motion amplitudes (A = 5, 10, 15, 20, 30, 40 and 50 mm) were used to create both ITV and RMI plans for each patient; this resulted in 14 treatment plans per patient, 252 plans in total. We only included the respiratory motion in the superior-inferior (SI) direction and the probability density functions (PDFs) describing the different motion amplitudes were based on a single motion trace (Figure 1). This way, the comparison
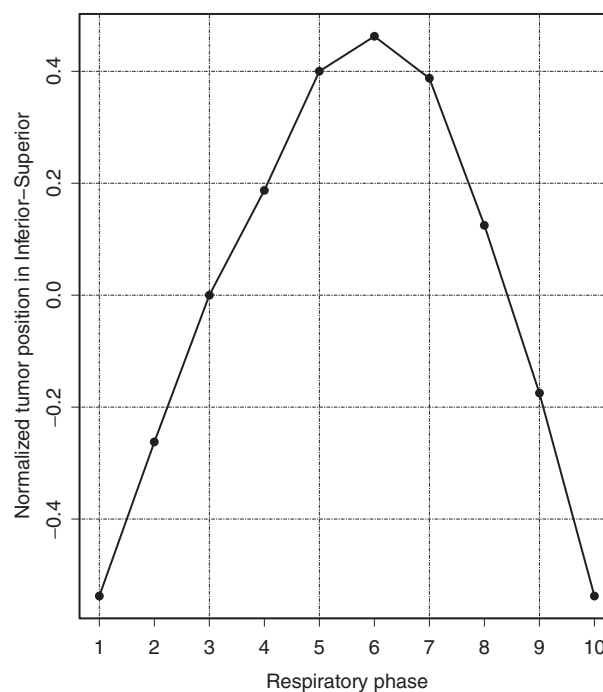


**Figure 1.** The motion trace describing the respiratory-induced tumor motion in inferior-superior direction for the 10 respiratory phases, as used for the simulated amplitudes. The motion trace is normalized to yield a peak-to-peak amplitude of 1; phase 1: end-inhale, phase 6: end-exhale.

between the ITV and RMI approach could be made solely as a function of the respiratory motion amplitude. Also, we expected the greatest effect to be in the SI direction because here the dose gradient was steepest due to the planar irradiation technique that was used. We used the motion trace that described the respiratory-induced tumor motion in the SI direction of patient 10. This motion trace described the tumor motion as typically observed in the clinic on the 10 phase scans of a 4DCT (i.e. a smooth continuous curve with the average tumor position in phase 2 and the exhale position in phase 6). The PDFs describing the different motion amplitudes were obtained by scaling the motion trace to simulate different peak-to-peak amplitudes. The probability of each tumor position was 0.1 and the tumor position in the respiratory phase that contains the tumor in its position closest to the mean position (i.e. tumor position in phase 2) was set to zero. To simulate the delivery of the treatment plan to a moving target (e.g. pancreatic tumor during free breathing) all dose distributions were convolved with the PDF that was also used for the treatment plan optimization, in order to obtain the final dose distributions [19].

To determine whether the RMI approach yielded clinically acceptable plans, we determined for each plan whether target coverage was obtained, with target coverage defined as $D_{98\%} \geq 95\%$ (i.e. the dose to 98% of the CTV should be at least 47.5 Gy).

The observed respiratory motion amplitude can vary substantially between what was observed at treatment planning and what was observed during daily treatment [3]. In an earlier study we observed that during 17% out of a total of 401 treatment fractions the motion amplitude differed $\geq 5$ mm compared to what was observed during treatment planning [3]. We investigated the extent to which the RMI plans were robust in terms of target coverage against the daily variations in tumor motion. We analyzed the effect on the target coverage of applying a different respiratory motion amplitude for the convolution of the optimized dose distribution (i.e. treatment delivery simulation) than was used for treatment plan optimization. As we used a single motion trace to describe tumor motion, and the main difference between patients was the tumor size, we demonstrated the robustness for the smallest (patient 12) and largest tumor (patient 17), only. For both patients, each of the seven dose distributions, optimized for a specific respiratory motion amplitude ranging from 5 to 50 mm, was convolved with eight PDFs (corresponding to amplitudes ranging from 0 to 50 mm), resulting in 56 different combinations per patient. For each combination, $D_{98\%}$ of the CTV was determined. We did not investigate the robustness against variations in the motion amplitude in all three directions as we expected the largest variations in the SI direction [3]. Also, because the dose gradient was steepest in the SI direction, variations in respiratory amplitudes in that direction will have the greatest effect on target coverage.

We systematically determined the difference in dose gradient steepness in the SI direction of the RMI approach compared to the ITV approach for respiratory motion amplitudes of up to 50 mm. We obtained the maximum distance in the inferior direction between the CTV and the 30 Gy isodose line

was determined in the coronal CT slice that contained the isocenter of the treatment plan and used as a measure for dose gradient steepness. This distance was chosen as a measure for gradient steepness because it also gave information on whether the high-dose volumes conformed to the CTV, whereas the distance between two isodose lines, which is often used to describe the dose gradient, does not. For each analyzed respiratory motion amplitude, the average and standard deviation of the steepness over all patients were determined and plotted, for ITV and RMI separately. For each motion amplitude, the statistical significance of the difference of the dose gradient steepness between the RMI and the ITV approach was tested using the Wilcoxon signed-rank test.

To illustrate the potential dosimetric benefit of using the RMI approach for the surrounding OARs, we analyzed the $D_{mean}$, $V_{30Gy}$, $V_{40Gy}$ and $V_{50Gy}$ of the duodenum for all ITV and RMI plans for patients 12 and 17 (i.e. smallest and largest tumor, respectively). We determined the differences in the four dosimetric parameters of the duodenum between the RMI and ITV approach for all simulated respiratory-induced motion amplitudes. The Wilcoxon signed-rank test was used to test whether these differences were statistically significant.

### Clinically observed three-dimensional motion amplitudes

To determine the benefit of the RMI approach compared to the ITV approach in a more clinical setting, we also created treatment plans using clinically observed respiratory motion amplitudes. Two treatment plans were made for each patient that were based on the 3D [i.e. SI, anterior-posterior (AP) and left-right (LR)] respiratory-induced motion as was observed on the clinically used pretreatment 4DCT scan; one using the ITV approach and one using the RMI approach. Again, all dose distributions were convolved with the PDF that was also used for the treatment plan optimization, to simulate the respiratory motion during treatment delivery [19].

To investigate the dosimetric benefit of the RMI approach for clinically observed respiratory motion amplitudes compared to the ITV approach, we determined the difference in dose to the duodenum. The duodenum was the OAR that was positioned closest to the PTV and for which the dose was expected to be influenced the most by a difference in dose gradient around the PTV. The $D_{mean}$, $V_{30Gy}$, $V_{40Gy}$ and $V_{50Gy}$ of the duodenum were analyzed for all ITV and RMI plans. The Wilcoxon signed-rank test was used to test whether these differences were statistically significant and Bland-Altman plots were created to visualize the differences.

### Results

### Simulated motion amplitudes

All RMI plans had good target coverage ($D_{98\%} > 95\%$) when the dose distribution was convolved with the same PDF as was used for the optimization procedure. Supplementary Figures B1(a–f) and B2(a–f) show, for patients 12 and 17, three examples of RMI dose distributions, for respiratory motion amplitudes of 5, 20 and 50 mm in the SI direction.
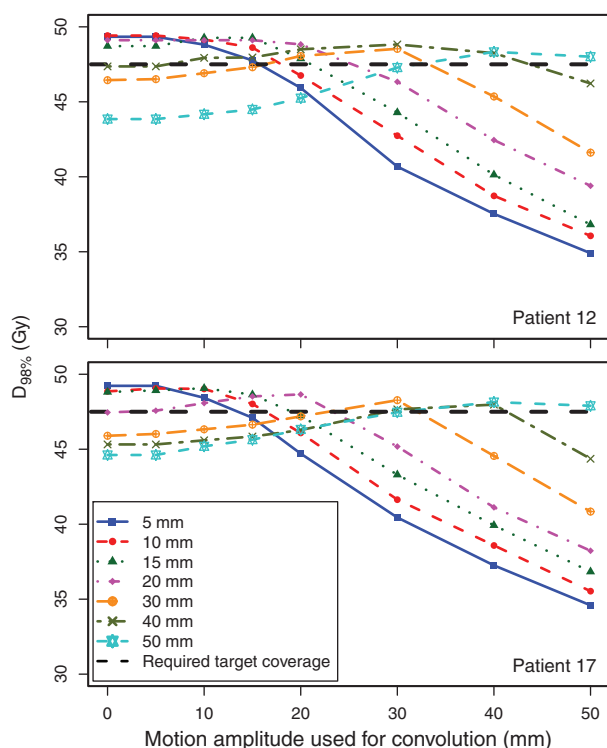
**Figure 2.** $D_{98\%}$ for the CTV as a function of the motion amplitude during treatment delivery simulation, for patient 12 (smallest tumor) and patient 17 (largest tumor), showing the robustness of the RMI treatment plans against daily variations in breathing amplitudes. For example, the solid blue lines represent $D_{98\%}$ for various breathing amplitudes for a plan that was optimized for a 5-mm breathing amplitude. The black dashed line represents the required target coverage ($D_{98\%} = 95\%$). The lines connecting the data points are a guide to the eye.

The static dose distributions (before convolution) can be highly inhomogeneous and the regions receiving high dose can extend to outside the target volume. After convolution, the distributions were homogeneous and conform to the CTV. For the ITV plans, the dose distributions were more conform to the CTV (Supplementary Figures B1(g–l) and B2(g–l)) after convolution.

The target coverage of the RMI plans was robust when the anticipated respiratory motion amplitude was ≤20 mm and the amplitude during treatment delivery was either ≤10 mm smaller or ≤5 mm larger (Figure 2). This was within the range of clinically expected amplitude variations.

The use of the RMI approach resulted in significantly (p ≤ .0002) steeper dose gradients for each simulated motion amplitude compared to the use of the ITV approach (Figure 3). A difference in the dose gradient of 1.7 mm (respiratory motion amplitude of 5 mm) up to 6.7 mm (amplitude of 50 mm) was observed. Both approaches show a strong linear relationship ($R^2 \geq .995$) between the respiratory motion amplitude and the steepness of the dose gradient. The small standard deviations in the distance over all 18 patients (error bars, Figure 3) indicate there is little effect of tumor volume on the steepness of the dose gradient around the CTV.

Table 1 shows the results for the evaluated dosimetric parameters of the duodenum for patients 12 and 17, for both the ITV and the RMI approach when using the simulated respiratory amplitudes. All parameters decreased
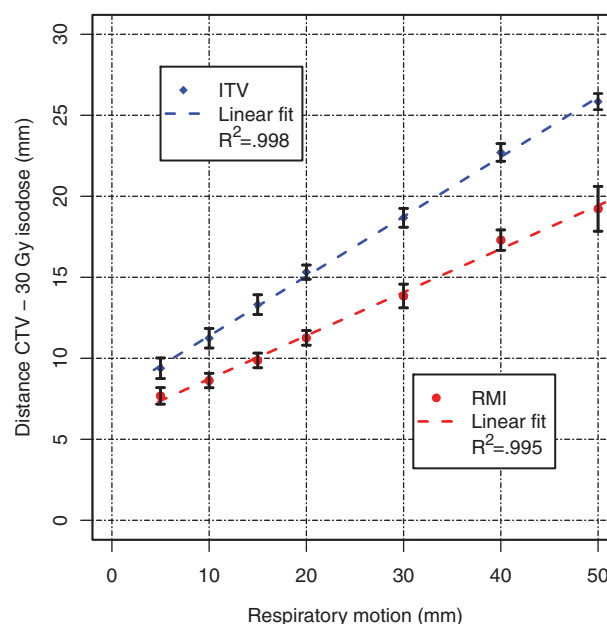


**Figure 3.** Steepness of the dose gradient in the superior-inferior direction, i.e. distance from the CTV to the 30 Gy isodose line, for the ITV and the RMI approach for the seven simulated respiratory motion amplitudes. Lines are linear fits to the mean values of each approach; error bars indicate the standard deviations over all 18 patients.

significantly (p ≤ .016), up to 51% for the $V_{50Gy}$ of patient 17 for a respiratory amplitude of 50 mm, when using the RMI instead of the ITV approach.

## Clinically observed three-dimensional motion amplitudes

The mean respiratory-induced motion amplitudes that were measured on the 4DCT and used to determine the clinical benefit were 2.4 (standard deviation 1.1; range 0.6–4.6) mm, 3.0 (1.0; 1.2–5.0) mm and 8.8 (3.3; 4.0–16.2) mm in LR, AP and SI, respectively. When applying these clinically observed respiratory motion amplitudes, the analyzed $D_{mean}$, $V_{30Gy}$, $V_{40Gy}$ and $V_{50Gy}$ parameters for the duodenum decreased by 0.43 Gy, 1.1 cm$^3$, 1.4 cm$^3$ and 0.9 cm$^3$, respectively (Figure 4). All differences, although statistically significant (p ≤ .009), were small and therefore not expected to have a high clinical impact.

## Discussion

The developed treatment planning approach prospectively incorporated respiratory motion of pancreatic tumors in the optimization of the treatment planning process and generated treatment plans that were directly deliverable by a treatment machine. The created treatment plans resulted in inhomogeneous dose distributions when delivered to a static target. To simulate respiratory motion during treatment delivery, the dose distributions were convolved with the expected tumor motion. After convolution, these RMI plans yielded good target coverage, steeper dose gradients and therefore significantly lower dose to surrounding OARs when compared to the use of an ITV. This is in agreement with earlier

**Table 1.** Dosimetric parameters for the duodenum for patients 12 and 17, for both the ITV and RMI approach (7 respiratory motion amplitudes each).

| | | ITV | | | | RMI | | | |
|---|---|---|---|---|---|---|---|---|---|
| | A (mm) | $D_{mean}$ (Gy) | $V_{30Gy}$ (cm³) | $V_{40Gy}$ (cm³) | $V_{50Gy}$ (cm³) | $D_{mean}$ (Gy) | $V_{30Gy}$ (cm³) | $V_{40Gy}$ (cm³) | $V_{50Gy}$ (cm³) |
| Patient 12 | 5 | 34.1 | 55.5 | 35.9 | 11.4 | 32.9 | 52.9 | 32.7 | 9.4 |
| | 10 | 35.6 | 58.7 | 38.8 | 12.8 | 33.6 | 53.9 | 33.1 | 10.2 |
| | 15 | 36.9 | 61.7 | 41.1 | 14.2 | 33.9 | 54.2 | 33.2 | 9.9 |
| | 20 | 38.0 | 64.3 | 43.1 | 14.7 | 35.8 | 59.8 | 36.5 | 8.9 |
| | 30 | 39.6 | 68.4 | 46.1 | 15.4 | 36.2 | 60.2 | 35.9 | 8.8 |
| | 40 | 40.7 | 72.5 | 48.7 | 15.7 | 38.2 | 67.5 | 40.0 | 8.1 |
| | 50 | 41.2 | 74.5 | 49.8 | 16.3 | 38.0 | 66.5 | 37.3 | 8.4 |
| Patient 17 | 5 | 42.4 | 87.9 | 69.4 | 35.5 | 40.9 | 83.0 | 63.7 | 31.0 |
| | 10 | 43.6 | 92.1 | 74.3 | 35.7 | 41.3 | 83.7 | 65.0 | 31.5 |
| | 15 | 44.8 | 96.8 | 78.9 | 39.9 | 41.8 | 86.6 | 65.9 | 30.9 |
| | 20 | 45.4 | 99.7 | 82.1 | 38.9 | 42.2 | 89.4 | 67.0 | 28.7 |
| | 30 | 46.2 | 101.8 | 87.2 | 40.7 | 43.1 | 94.6 | 70.3 | 27.8 |
| | 40 | 46.6 | 102.3 | 90.3 | 39.7 | 43.5 | 97.5 | 71.8 | 26.5 |
| | 50 | 46.8 | 102.5 | 92.2 | 40.8 | 43.5 | 99.9 | 71.8 | 20.0 |

A: respiratory motion amplitude; ITV: internal target volume; Pat: patient; RMI: respiratory motion-incorporated.
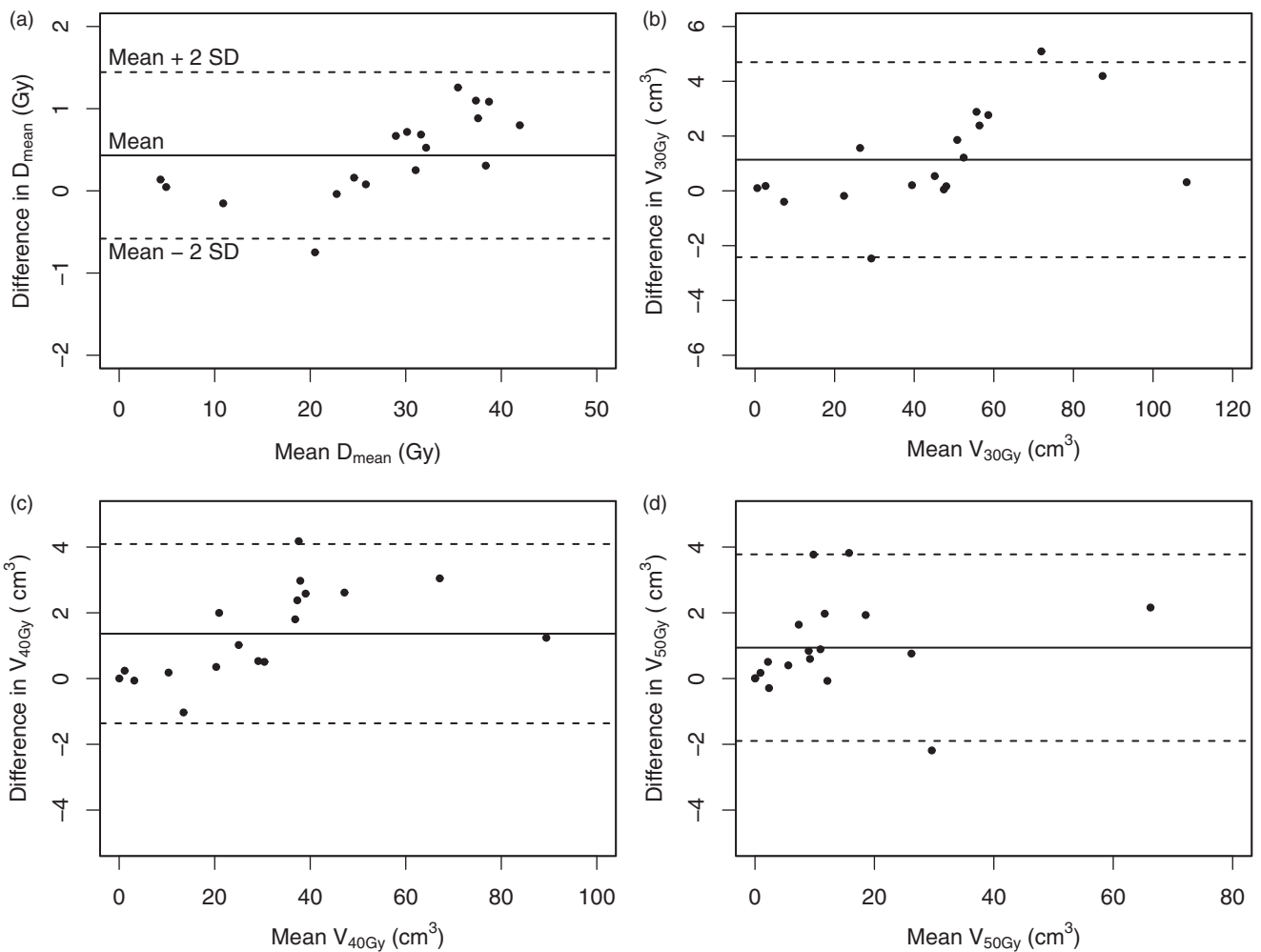


**Figure 4.** Bland-Altman plots for the duodenum, showing for each dosimetric parameter the difference (i.e. ITV value minus RMI value) for all 18 patients. The clinically observed three-dimensional motion amplitudes were used.

results from the literature where the inferiority of the ITV was shown for a lung and a liver case [15]. However, for clinically observed respiratory-induced motion amplitudes, the differences in dose to the duodenum, which was in close proximity to the PTV and expected to be affected most by a change in the dose gradient, were small.

An earlier study showed that in clinical practice, 4DCT overestimates the respiratory-induced motion amplitude compared to the daily tumor motion for the majority of patients [3]. This overestimate was typically in the range of 5–10 mm, with the amplitudes in the SI direction on 4DCT typically ≤20 mm. The current study shows that the RMI

Before convolution:
Optimized for 20 mm

After convolution:
Blurred with 10 mm
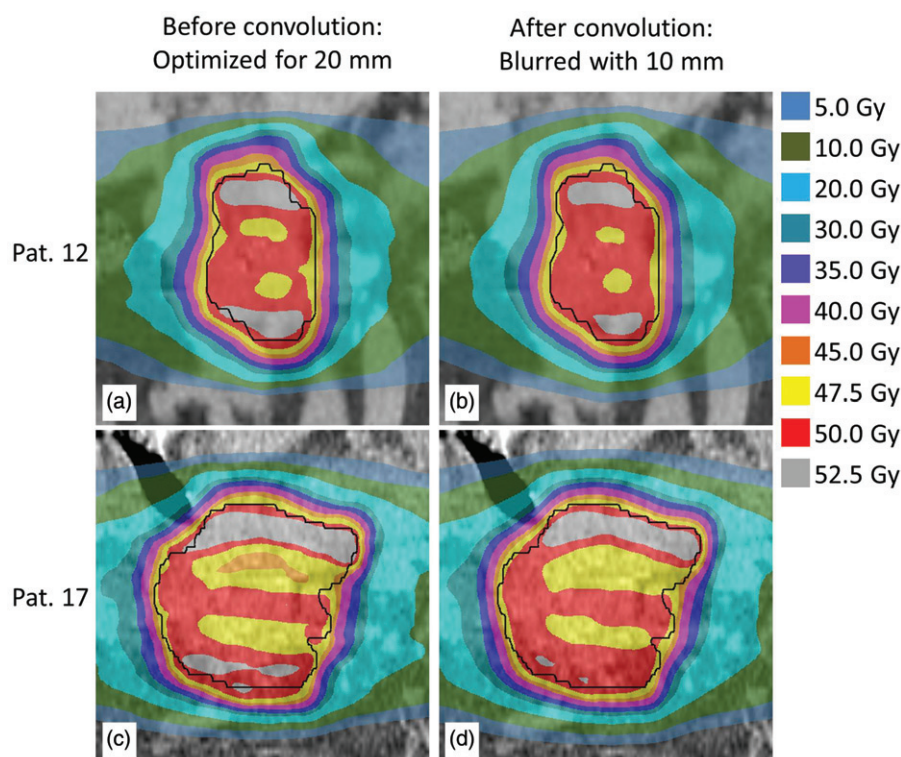


**Figure 5.** For patients 12 (top) and 17 (bottom), dose distribution optimized for a simulated respiratory amplitude of 20 mm using the RMI approach (a and c) and the same distributions convolved with the PDF describing a simulated respiratory motion amplitude of 10 mm (b and d).

approach yielded clinically acceptable plans for moving targets that had a motion amplitude of up to 50 mm in the SI direction. In a clinical setting this approach would result in treatment plans that are robust in terms of target coverage against expected variations in respiratory amplitude, although the dose inhomogeneity might increase (Figure 5). The ITV approach, inherently, will always yield sufficient target coverage and a homogeneous dose distribution when the motion amplitude during treatment is smaller than the amplitude used to create the ITV.

This study only considered rigid motion patterns, which limited the ability to accurately determine the benefit of using a probabilistic treatment planning approach for radiotherapy of pancreatic cancer. The developed approach can be extended to include anatomical deformations as well. However, the effects of deformations are expected to be minimal as it has been shown that the dosimetric differences, for both the target volume and healthy tissues, between using deformable image registration compared to rigid body translations are small in the upper abdominal region [20]. The interplay effect between treatment delivery over time and tumor motion was neglected as this does not affect the delivered dose [21].

The RMI approach resulted in a significant reduction of dose to the duodenum when compared to the ITV approach. High-dose volumes ($V_{55Gy} > 1\,cm^3$ and $V_{50Gy} > 16\,cm^3$) of the duodenum have been identified as strong predictors for toxicity [22,23]. The steeper dose gradient obtained by the RMI approach reduces these high-dose volumes, as was shown in this study. As the duodenum overlapped with the PTV for all patients, using the maximum dose as an evaluation

parameter was not suitable to evaluate the difference between the ITV and RMI approach.

In an earlier study we showed that the use of a mid-ventilation approach for irradiation of pancreatic tumors can significantly reduce the dose to surrounding OARs while maintaining sufficient target coverage [18]. However, in the RMI approach the treatment planning system has the additional freedom to create initially inhomogeneous dose distributions, which can result in steep dose gradients in the final convolved dose distribution. The mid-ventilation approach merely applies smaller margins than the ITV approach and thus creates a homogeneous dose distribution. However, because in this study we compared the RMI approach to the ITV (a highly conservative technique) and we only observed minimal dosimetric gain, we expect the dosimetric difference between the mid-ventilation and RMI approach to be small. Further research is needed to determine which technique might be better in terms of robustness against variations in the respiratory amplitude and reducing the dose to OARs.

RMI planning and treatment requires accurate alignment of the mean tumor position during treatment with the expected mean tumor position from the planning CT scan. As a result of the more conformal dose distributions compared to the use of an ITV, the dosimetric impact of a mismatch might be larger for the RMI approach. It is therefore recommended to daily position the patient by registration of the mean tumor position obtained from a daily 4D-CBCT with the mean tumor position during respiration obtained from a pretreatment 4DCT combined with the use of intratumoral fiducials. For this daily position verification, small (i.e. ø = 0.28–0.35 mm) intratumoral fiducials that can be

implanted during a endoscopic procedure can be used [1,2,24].

Our results show that our newly developed approach of prospectively incorporating respiratory-induced pancreatic tumor motion in the optimization process can yield more conformal dose distributions compared to the ITV approach. However, the dosimetric gain highly depends on the respiratory-induced motion amplitude; for the 18 patients for whom treatment plans were based on the clinical amplitudes, we observed only small differences in dose to the duodenum. When the respiratory motion amplitude becomes larger (i.e. >15 mm) the dosimetric benefit becomes more substantial. In daily clinical practice, treatment planning combined with probabilistic optimization will likely result in only a minimal clinical gain and for each treatment site it should be determined what this gain on average would be. For pancreatic cancer patients, we recommend using a probabilistic planning strategy only when the respiratory-induced motion amplitude is >15 mm, which might occur in only a limited number of patients. For smaller amplitudes using a simple expansion of the target volume to account for the respiratory motion may be sufficient.

In conclusion, prospective incorporation of respiratory-induced pancreatic tumor motion in the treatment plan optimization process resulted in treatment plans that had good target coverage and were robust against variations in the respiratory motion amplitude within a certain bandwidth. Probabilistic treatment plans had significantly steeper dose gradients and therefore yielded significantly lower dose to surrounding OARs compared to the use of an ITV. However, the potential clinical gain of this treatment planning technique for this patient group was limited.

## Disclosure statement

## Funding

## References

[1] van der Horst A, Wognum S, Dávila Fajardo R, et al. Interfractional position variation of pancreatic tumors quantified using intratumoral fiducial markers and daily cone beam computed tomography. Int J Radiat Oncol Biol Phys. 2013;87:202–208.

[2] van der Horst A, Lens E, Wognum S, et al. Limited role for biliary stent as surrogate fiducial marker in pancreatic cancer: stent and intratumoral fiducials compared. Int J Radiat Oncol Biol Phys. 2014;89:641–648.

[3] Lens E, van der Horst A, Kroon PS, et al. Differences in respiratory-induced pancreatic tumor motion between 4D treatment planning CT and daily cone beam CT, measured using intratumoral fiducials. Acta Oncol. 2014;53:1257–1264.

[4] Mutaf YD, Brinkmann DH. Optimization of internal margin to account for dosimetric effects of respiratory motion. Int J Radiat Oncol Biol Phys. 2008;70:1561–1570.

[5] Verellen D, Depuydt T, Gevaert T, et al. Gating and tracking, 4D in thoracic tumours. Cancer Radiother. 2010;14:446–454.

[6] Heerkens HD, van Vulpen M, van den Berg CAT, et al. MRI-based tumor motion characterization and gating schemes for radiation therapy of pancreatic cancer. Radiother Oncol. 2014;111:252–257.

[7] Li JG, Xing L. Inverse planning incorporating organ motion. Med Phys. 2000;27:1573–1578.

[8] Birkner M, Yan D, Alber M, et al. Adapting inverse planning to patient and organ geometrical variation: algorithm and implementation. Med Phys. 2003;30:2822–2831.

[9] Unkelbach J, Oelfke U. Inclusion of organ movements in IMRT treatment planning via inverse planning based on probability distributions. Phys Med Biol. 2004;49:4005–4029.

[10] Chan TCY, Bortfeld T, Tsitsiklis JN. A robust approach to IMRT optimization. Phys Med Biol. 2006;51:2567–2583.

[11] Moore JA, Gordon JJ, Anscher MS, et al. Comparisons of treatment optimization directly incorporating random patient setup uncertainty with a margin-based approach. Med Phys. 2009;36:3880–3890.

[12] Moore JA, Gordon JJ, Anscher MS, et al. Comparisons of treatment optimization directly incorporating systematic patient setup uncertainty with a margin-based approach. Med Phys. 2012;39:1102–1111.

[13] Bohoslavsky R, Witte MG, Janssen TM, et al. Probabilistic objective functions for margin-less IMRT planning. Phys Med Biol. 2013;58:3563–3580.

[14] Jin J-Y, Ajlouni M, Kong F-MS, et al. Utilize target motion to cover clinical target volume (ctv)–a novel and practical treatment planning approach to manage respiratory motion. Radiother Oncol. 2008;89:292–303.

[15] Trofimov A, Rietzel E, Lu H-M, et al. Temporo-spatial IMRT optimization: concepts, implementation and initial results. Phys Med Biol. 2005;50:2779–2798.

[16] Söhn M, Weinmann M, Alber M. Intensity-modulated radiotherapy optimization in a quasi-periodically deforming patient model. Int. J Radiat Oncol Biol Phys. 2009;75:906–914.

[17] Heath E, Unkelbach J, Oelfke U. Incorporating uncertainties in respiratory motion into 4D treatment plan optimization. Med Phys. 2009;36:3059–3071.

[18] Lens E, van der Horst A, Versteijne E, et al. Dosimetric advantages of midventilation compared with internal target volume for radiation therapy of pancreatic cancer. Int J Radiat Oncol Biol Phys. 2015;92:675–682.

[19] Bel A, van Herk M, Lebesque JV. Target margins for random geometrical treatment uncertainties in conformal radiotherapy. Med Phys. 1996;23:1537–1545.

[20] Velec M, Moseley JL, Eccles CL, et al. Effect of breathing motion on radiotherapy dose accumulation in the abdomen using deformable registration. Int J Radiat Oncol Biol Phys. 2011;80:265–272.

[21] Bortfeld T, Jokivarsi K, Goitein M, et al. Effects of intra-fraction motion on IMRT dose delivery: statistical analysis and simulation. Phys Med Biol. 2002;47:2203–2220.

[22] Nakamura A, Shibuya K, Matsuo Y, et al. Analysis of dosimetric parameters associated with acute gastrointestinal toxicity and upper gastrointestinal bleeding in locally advanced pancreatic cancer patients treated with gemcitabine-based concurrent chemoradiotherapy. Int J Radiat Oncol Biol Phys. 2012;84:369–375.

[23] Kelly P, Das P, Pinnix CC, et al. Duodenal toxicity after fractionated chemoradiation for unresectable pancreatic cancer. Int J Radiat Oncol Biol Phys. 2013;85:e143–e149.

[24] Dávila Fajardo R, Lekkerkerker SJ, van der Horst A, et al. EUS-guided fiducial markers placement with a 22-gauge needle for image-guided radiation therapy in pancreatic cancer. Gastrointest Endosc. 2014;79:851.